JOURNAL OF VIROLOGY, May 1986, p. 426–433
0022-538X/86/050426-08$02.00/0

Vol. 58, No. 2

Restricted Replication of Mouse Hepatitis Virus A59 in Primary Mouse Brain Astrocytes Correlates with Reduced Pathogenicity

MARIO F. VAN BERLO,[1]* GUUS WOLSWIJK,[1] JERO CALAFAT,[2] MARCK J. M. KOOLEN,[1] MARIAN C. HORZINEK,[1] AND BERNARD A. M. VAN DER ZEIJST[1]

Institute of Virology, Veterinary Faculty, State University, 3508 TD Utrecht,[1] and The Netherlands Cancer Institute, Antoni van Leeuwenhoekhuis, 1066 CX Amsterdam,[2] The Netherlands

Received 29 July 1985/Accepted 31 December 1985

Temperature-sensitive (*ts*) mutants of mouse hepatitis virus A59 (MHV-A59) are drastically attenuated in their pathogenic properties. Intracerebral inoculation of mice with 10^5 PFU of mutant *ts*342 results in prolonged infection of the central nervous system, whereas 100 PFU of wild-type virus are lethal (M. J. M. Koolen, A. D. M. E. Osterhaus, G. van Steenis, M. C. Horzinek, and B. A. M. van der Zeijst, Virology 125:393–402, 1983). In the Sac(−) cell line *ts*342 grows as well at 37°C (the body temperature of mice) as at 31°C (the permissive temperature). There is, however, a difference in primary cultures of mouse brain astrocytes. After infection with *ts*342, astrocytes produced low levels of infectious virus (5.2 ± 3.7%) compared with virus yields after infection with wild-type virus. The fraction of wild-type virus- and *ts*342-infected cells was similar. Electron microscopy showed in wild-type virus-infected cells abundant virions in smooth vesicles usually closely associated with a well-developed Golgi apparatus. In mutant-infected cells no mature *ts*342 virus particles were found. There was no difference between *ts*342 and wild-type virus regarding the intracellular virus-specific RNAs. In *ts*342-infected cells the viral glycoproteins E2 and E1 were not detectable or were barely detectable. Either the mRNAs for the glycoproteins are not translated or the proteins are rapidly broken down. Revertants of *ts*342 were isolated. They grew as well as wild-type virus in astrocytes, indicating that (i) they apparently produced sufficient amounts of E2 and E1, (ii) the *ts* defect itself rather than a second site mutation is responsible for the defect in replication, and (iii) the *ts* defect acts in unison with host-cell factors. The revertants also regained the lethal properties of wild-type virus.

Murine coronaviruses have been used to study virus-induced chronic demyelinating disease (36). Most investigations have been carried out with the JHM strain of mouse hepatitis virus (MHV), isolated from mice with hind-leg paralysis (4). JHM and other MHV strains occur endemically in mouse colonies, many of which have antibodies against MHV (7, 27). The clinical picture varies from hepatitis and, in young mice, enteric infection to neurological disease (36). Experimental infection with the original JHM strain was found to cause demyelination (1).

Immunologically naive mice die from acute encephalomyelitis after infection with high virus doses of MHV, whereas low doses do not infect all animals; this experimental problem has been overcome by the use of temperature-sensitive (*ts*) mutants. Haspel et al. (10) have shown that high doses of a particular mutant (*ts*8) of MHV-JHM are not lethal but lead to a high incidence of demyelination. This mutant differs from wild-type virus in that it does not infect neurons but only nonneuronal cells such as oligodendrocytes and astrocytes (6, 14).

We chose strain A59 (MHV-A59) to study the interaction of this virus with cells of the central nervous system. MHV-A59 was isolated from mice with hepatic disease (19); at the moment it is undoubtedly the best-characterized coronavirus (26, 28, 31, 33). Lavi et al. (17) demonstrated that wild-type MHV-A59 is also neurotropic after experimental infection. Koolen et al. (15) showed that some *ts* mutants of MHV-A59 no longer cause acute fatal encephalitis in mice but instead cause prolonged demyelinating disease. The mutants have been induced chemically, but similar mutations might arise in nature, owing to the hypermutability of RNA genomes (11).

One mutant (*ts*342) has been studied in more detail. Demyelination was observed as early as 3 days after intracerebral inoculation (M. J. M. Koolen, W. Wouda, J. Calafat, M. C. Horzinek, and B. A. M. van der Zeijst, submitted for publication). Surprisingly, in Sac(−) cells, a permanent cell line, *ts*342 grew equally well at 37°C (the body temperature of mice) and at 31°C (the permissive temperature); the *ts* defect only became apparent between 37°C and the restrictive temperature (40°C). The aim of the present study was to characterize in more depth the interaction between *ts*342 and cells of the nervous system. Since primary brain cultures consisting of different types of brain cells did not have one specific target cell for *ts*342 (M. J. M. Koolen, J. Calafat, W. Wouda, M. F. van Berlo, M. C. Horzinek, and B. A. M. van der Zeijst, submitted for publication), we chose astrocytes as an initial approach. Astrocytes play an important role in the functioning brain and can be obtained in pure cultures (9).

MATERIALS AND METHODS

Cells and viruses. Mouse L cells obtained from F. Lehmann-Grube, Hamburg, Federal Republic of Germany, and Sac(−) cells, a Moloney sarcoma virus-transformed cell line defective in virus production (37), were grown in Dulbecco modified Eagle medium containing 10% fetal calf serum and supplemented with 100 IU of penicillin per ml and 100 μg of streptomycin per ml (DMEM–10% FCS).

Primary cultures of dissociated central nervous system

* Corresponding author.

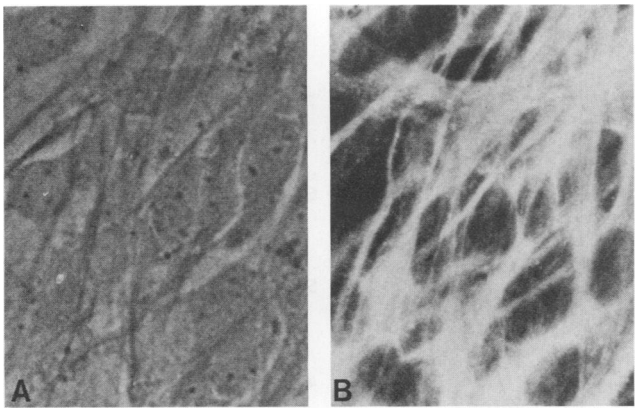

FIG. 1. Seven-day-old primary cultures prepared from 14-day-old embryonal mouse brains. The same field was photographed twice: (A) phase-contrast microscopy; (B) indirect immunofluorescence staining for glial fibrillary acidic protein.

cells were obtained from the cerebral hemispheres of approximately 14-day-old BALB/c mouse embryos. The sera of the pregnant mice used (Centraal Proefdierenbedrijf, TNO, Zeist, The Netherlands) were shown to be negative for anti-MHV antibodies both in a plaque reduction assay and in an immunofluorescence assay (29). Brains of about eight fetuses were rinsed in phosphate-buffered saline (PBS), and meningeal material was removed. A cell suspension was obtained by mechanical dissociation. About 10^6 cells were suspended in DMEM–10% FCS supplemented with 10% heat-inactivated horse serum and 80 IU of insulin per liter and seeded on glass cover slips (18 by 18 mm) in 35-mm petri dishes. Cultures were maintained at 37°C in a CO_2 incubator at 100% humidity for 7 days. During this period, the cells were refed twice the fresh medium. Virus stocks of MHV-A59 and *ts*342 were prepared as described previously (15).

Virus was plaque titrated on L cells (15) with an overlay containing 1.5% Bacto-Agar (Difco Laboratories, Detroit, Mich.) in DMEM–1% FCS. Plaques were read after 1 day at 37°C or 2 days at 31°C.

Kinetics of virus growth. Sac(−) cells and brain cells, grown on cover slips (10 by 10 mm) in 16-mm tissue culture clusters were infected at a density of 4×10^5 cells with 50 PFU per cell in 0.1 ml of DMEM–3% FCS. After 1 h at 37°C, the inoculum was removed and replaced by 1 ml of DMEM–10% FCS after washing the cells twice with DMEM. At 2 h postinfection (p.i.), the cells were washed again, and fresh medium was added. Culture fluids were collected at appropriate intervals, and infectious virus was assayed by plaque titration.

Antisera and indirect immunofluorescence. Anti-MHV-A59 serum raised in a rabbit (25) or in mice (30) was used. Both sera recognize the nucleocapsid protein and the two viral glycoproteins, E1 and E2. Rabbit anti-glial fibrillary acidic protein serum was a gift of M. C. Raff, University College London, United Kingdom. For fluorescent-antibody staining, cover slip cultures were fixed in 5% acetic acid in ethanol at −20°C for 10 min. After washing with PBS, the cells were incubated for 30 min with the immunoglobulin G (IgG) fraction from the rabbit anti-MHV-A59 serum (1:30 dilution in PBS) or with anti-glial fibrillary acidic protein serum (1:200), followed by extensive rinsing with PBS and a further incubation for 30 min with fluorescein isothiocyanate-labeled sheep IgG directed against rabbit IgG (1:50) (Miles-Yeda Ltd., Rehovot, Israel). After washing in PBS, the cover slips were mounted in PBS-glycerol (1:1).

Electron microscopy. Brain cells were grown in 35-mm tissue culture dishes and infected as described above. At 26 h p.i. an equal volume of fixative (2.5% glutaraldehyde in 0.1 M cacodylate buffer, pH 7.2) was added to the medium. After washing with cacodylate buffer, the cells were postfixed for 1 h in 1% osmium tetroxide in the same buffer. The monolayers were scraped off the dishes with a rubber policeman, pelleted by centrifugation, dehydrated, and embedded in a mixture of Epon and Araldite. Thin sections were stained with uranyl acetate and lead hydroxide and examined with a Philips EM 301 electron microscope.

Analysis of virus-specific proteins and RNAs in cells infected with wild-type MHV-A59 and *ts*342. Sac(−) and brain cells grown on cover slips (20 by 20 mm) in 35-mm tissue culture dishes were infected as described above. For protein labeling Sac(−) cells were labeled from 7 to 9 h p.i. and brain cells were labeled from 22 to 24 h p.i. with 1 ml of methionine-deficient minimal essential medium supplemented with 5% FCS and 25 μCi of [^{35}S]methionine (1,230 Ci/mmol; The Radiochemical Centre, Amersham, United Kingdom). After the labeling period, the cover slips were rinsed with cold PBS, and the cells were lysed for 5 min in 0.15 ml of lysis buffer (15). Lysates were centrifuged for 5 min at 10,000 × *g* and then processed directly or stored at −70°C.

Virus-specific proteins were immunoprecipitated from 75-μl portions of the lysates with 10 μl of mouse anti-MHV-A59 serum by previously described methods (15). To reduce the aspecific background in immunoprecipitates of infected brain cells, lysates were preincubated with 10 μl of antigalactocerebroside serum and 200 μl of a 10% *Staphylococcus aureus* suspension before virus-specific proteins were immunoprecipitated. Samples were electrophoresed in 15% acrylamide–0.085% bisacrylamide gels (25). Proteins were visualized by fluorography on preflashed Fuji RX film at −70°C (16).

For RNA analysis, the cells were incubated in the presence of 1 μg of actinomycin D per ml starting 6 h p.i. for Sac(−) cells or 15 h p.i. for brain cells. One hour later, [^{3}H]uridine (50 μCi/ml, 28 Ci/mmol; The Radiochemical Centre) was added, and the cells were labeled until 9 or 22 h p.i. for Sac(−) or brain cells, respectively. After this period, they were washed, and RNA was isolated by phenol extraction as described previously (13). RNAs were glyoxal denaturated and analyzed by electrophoresis in urea-containing agarose gels (30).

Isolation of revertants of *ts*342. *ts*342 was plaque titrated at 40°C with an overlay containing 0.4% agarose (E. Merck AG, Darmstadt, Federal Republic of Germany). Well-isolated plaques were removed, diluted in 0.5 ml of DMEM–3% FCS, and replaqued at both 31 and 40°C. One isolate with similar titers at both temperatures was recloned, and a stock was prepared. Two other revertants were isolated and recloned by endpoint-dilution titration at 40°C. Plaque titration of *ts*342 at 40 and 31°C gave a ratio of about 10^{-5}, compared with 1.5 to 8 for the revertants or wild-type virus.

RESULTS

Primary brain cell cultures. The embryonal mouse brain cell cultures reached confluency after about 7 days. Figure 1 shows that most of the cells in the cultures (80 to 90%) were positive for glial fibrillary acidic protein, an astrocyte marker (2). Some neurons could be demonstrated by Nissl staining, and a few microglial-like cells filled with cell debris were

observed. Oligodendrocytes could not be detected in these cultures by staining with antigalactocerebroside serum.

Kinetics of virus growth and synthesis of viral antigens. MHV-A59 and *ts*342 virus had similar single-cycle kinetics of virus growth in Sac(−) cells at 37°C (Fig. 2A). Also, the amount of viral antigen and the percentage of infected cells, as detected by immunofluorescence, were similar in cells infected with both virus strains. At 4 h p.i. viral antigen was first observed; small syncytia appeared 2 h later. At 10 h p.i. all the cells had fused.

In mouse brain cells the production of infectious wild-type MHV-A59 and *ts*342 followed different kinetics (Fig. 2B). A maximum virus yield of wild-type virus was obtained at 20 h p.i. *ts*342 grew at a slower rate than wild-type virus, and final virus titers were much lower. Although the astrocyte cultures were infected at a multiplicity of infection of 50, the fraction of antigen-containing cells was initially much smaller than in Sac(−) cells. Apparently the astrocyte cultures were more resistant to infection with both wild-type virus and *ts*342. With increasing time after infection, all cells eventually became antigen positive (Table 1). There was no difference in the intracellular distribution of antigens in cells injected with wild-type or mutant virus. The increase in antigen-positive cells could be the result of multiple cycles of replication of both viruses in astrocytes. Such an assumption is supported by the kinetics of production of extracellular virus (Fig. 2B).

The progeny yield of infectious *ts*342 varied somewhat between experiments. It could be as low as 1.4% compared with that of wild-type virus. The average of four experiments was 5.2 ± 3.7%. This residual yield was still temperature sensitive and thus not due to revertants. It might be progeny from the small fraction of other cell types present in the cultures.

The low yield of infectious virus from *ts*342-infected astrocytes, while viral antigens were distributed in the same way and present in the same fraction as in wild type-infected astrocytes, suggests that there is a defect in the maturation of *ts*342 in astrocytes.

Electron microscopy of virus-infected mouse brain cells. In wild-type virus-infected cells virus particles were abundant (Fig. 3). Budding and free virions were detected in cisternae of smooth membranes. Free virions resembling those seen in vacuoles were also observed in the extracellular space. In all virus particles the nucleocapsid was visible, consisting of electron-dense granularlike material almost completely filling the viral core (Fig. 3a) (20). Tubular bodies, as described by David-Ferreira and Manaker (5), consisting of smooth membrane were observed in the cytoplasm. In *ts*342-infected cells no virus particles were seen. In some cells, however, a system of cytoplasmic sheets of smooth membranes was present along with spherical particles with a diameter of about 70 nm consisting of two concentric membranes (Fig. 4). The core of these particles had no granular like material resembling the nucleocapsid of MHV. These particles did not resemble any known retroviruses (32), but it cannot be excluded that they represent cross-sections of tubular arrays of membranes. None of these structures, i.e., sheets of membranes and spherical particles, were found in mock-infected cells.

TABLE 1. Fraction of primary mouse brain cells (astrocytes) expressing viral antigens after infection with wild-type MHV-A59 or mutant *ts*342

h p.i.	% Positive cells[a]	
	Wild type	*ts*342
8	5	1
16	10	5
24	75	40
32	99	95

[a] Assayed by immunofluorescence with rabbit anti-MHV-A59 serum.

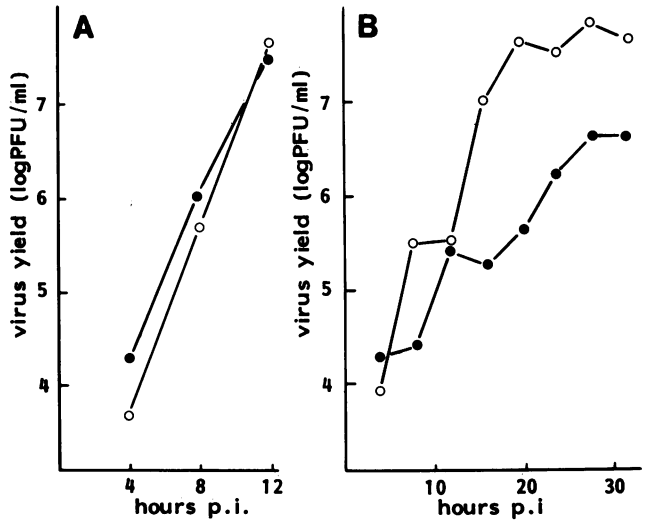

FIG. 2. Kinetics of virus growth in Sac(−) cells (A) and primary mouse brain astrocytes (B) infected with wild-type MHV-A59 (○) and *ts*342 (●). Cells were infected with 50 PFU per cell. At various times p.i. samples of the culture fluid were taken in which infectious virus was assayed by plaque titration at 31°C.

Virus-specific intracellular protein synthesis. An explanation for the defect in maturation of *ts*342 in mouse brain cells would be a defect in the synthesis of one or more viral proteins. Therefore, infected Sac(−) cells and mouse astrocytes were labeled with [^{35}S]methionine. Virus-specific intracellular proteins were immunoprecipitated from infected cells and analyzed by polyacrylamide gel electrophoresis. In infected Sac(−) cells no difference in intracellular virus-specific protein synthesis was observed between wild-type virus and *ts*342. All virus-specific polypeptides were labeled with [^{35}S]methionine: gp150/E2; pp54/N and its degradation products (23); gp26.5/E1; gp25.5/E1; p24/E1; and p22, a minor virion protein (24) (Fig. 5).

Mouse brain cells infected with wild-type virus contained the same set of virus-specific proteins as infected Sac(−) cells when pulse-labeled between 16 and 30 h p.i. *ts*342-infected astrocytes, however, lacked any detectable E2 and p24/E1, while very little gp26.5/E1 and gp25.5/E1 were observed. The results of the labeling between 22 and 24 h p.i. are shown in Fig. 5. They suggest that the defect in virus maturation in *ts*342-infected brain cells, as detected by electron microscopy, is due to the absence or near absence of the viral glycoproteins.

Virus-specific intracellular RNA synthesis. A lack of synthesis of the viral glycoproteins could be due to the absence of RNA 3 and RNA 6, encoding the E2 and E1 glycoproteins, respectively (25). Infected mouse brain cells were labeled with [^{35}H]uridine in the presence of actinomycin D from 16 to 22 h p.i. The levels of virus-specific RNA synthesis in wild-type (100%)- and *ts*342 (75%)-infected cells were comparable. The RNAs were isolated and analyzed by

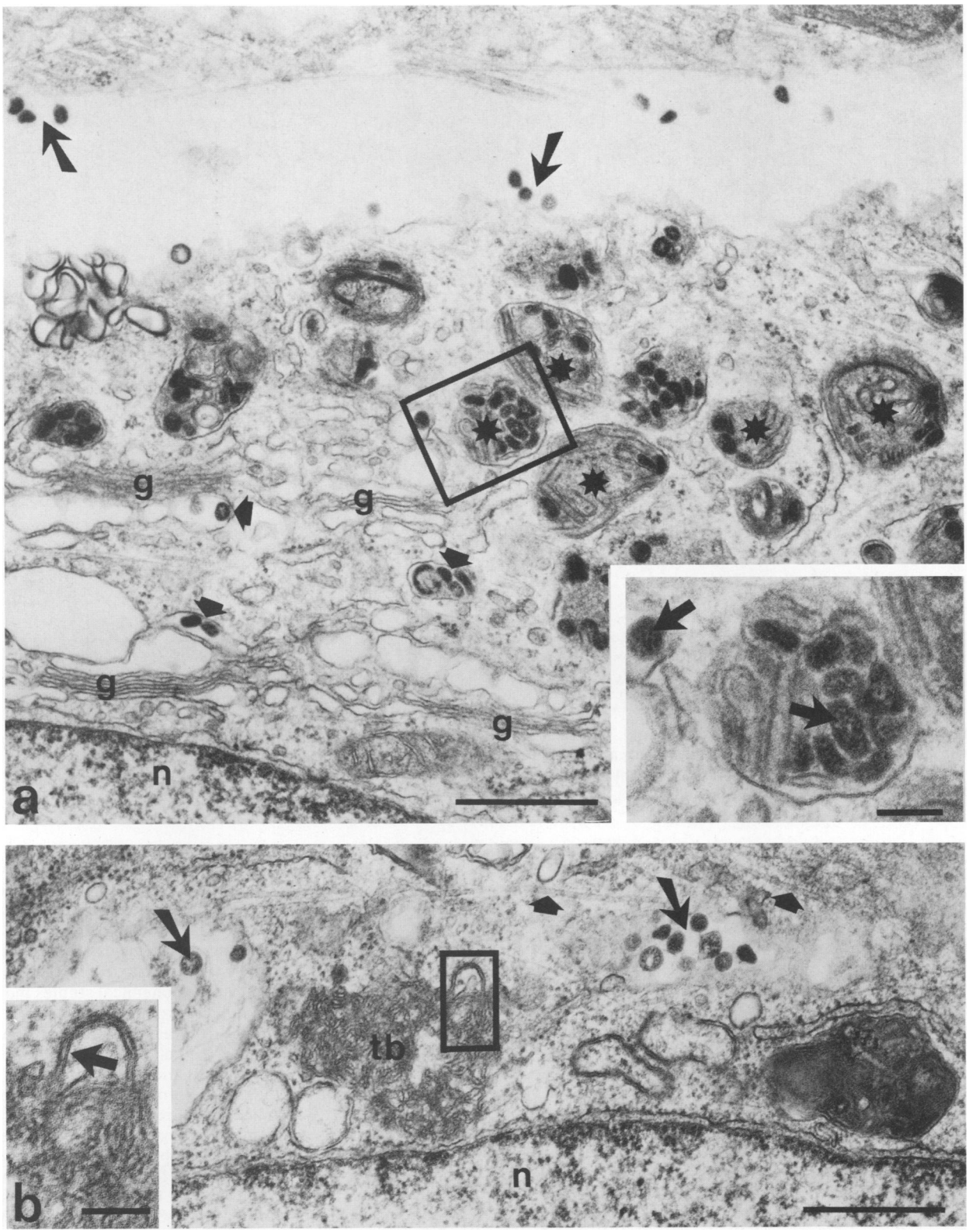

FIG. 3. Wild-type virus-infected brain astrocytes 26 h p.i. (a) Budding and free virions are seen in vesicles (small arrows) associated with the Golgi apparatus (g). Smooth-membrane vesicles containing virions and tubular structures (asterisks) are abundant; free virus (large arrows) is found in the extracellular space. n, Nucleus. Inset: Higher magnification of the marked area showing virions with electron-dense granular like material filling the viral core (arrows). (b) Tubular body (tb) and microtubules (small arrows) are shown in the cytoplasm. Virions (large arrows) are present in vacuoles. n, Nucleus. Inset: Higher magnification of the marked area showing the tubular body consisting of smooth membranes (arrow). Bars: 0.5 μm and 0.1 μm (inset).

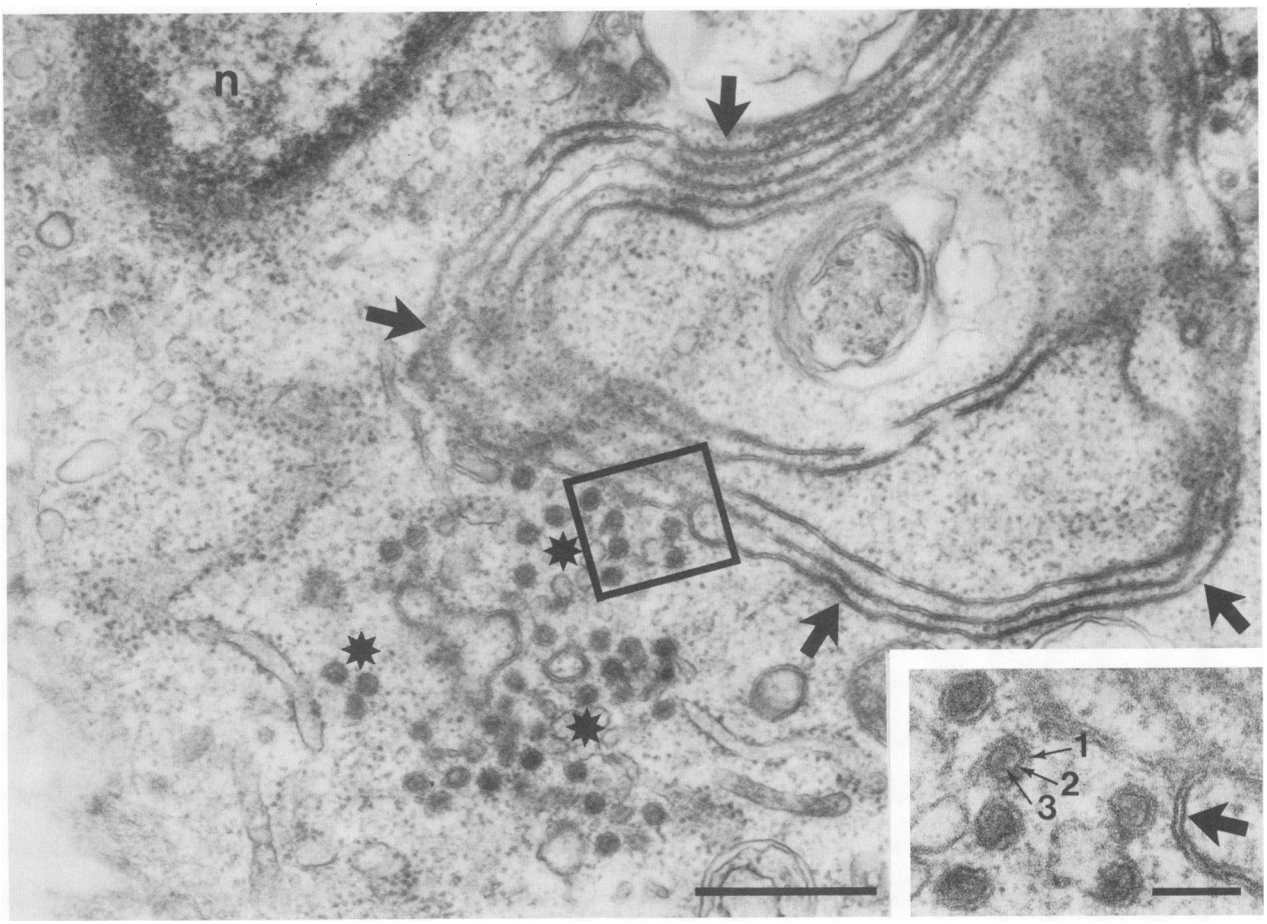

FIG. 4. *ts*342-infected brain astrocytes 26 h p.i. A system of membrane sheets is shown in the cytoplasm (arrows) along with spherical particles (asterisks). n, Nucleus. Inset: Higher magnification of the marked area showing the sheets consisting of smooth membrane (arrow) and the particles consisting of an outer (1) and inner (2) membrane surrounding a core (3) devoid of electron-dense granularlike material. Compare these particles with the virions of Fig. 3. Bars; 0.5 μm and 0.1 μm (inset).

agarose gel electrophoresis. No difference was observed between the viral RNAs in wild-type virus- and *ts*342-infected cells (Fig. 6).

Is the restricted growth of *ts*342 in astrocytes due to its *ts* defect or to a second site mutation? *ts*342 is an RNA^- mutant, unable to synthesize virus-specific RNAs at 40°C in tissue cultures cells. A priori it is not clear how such a mutation would manifest itself in astrocytes by the selective disappearance of the viral glycoproteins. Therefore, this effect could well be due to another, non-*ts* mutation. Such lesions can be expected to arise after chemical mutagenesis.

Three revertants of *ts*342 were isolated. The 26-h virus yield of these revertants in astrocytes was determined. On average it was comparable to that of wild-type virus and 65-fold higher than that of *ts*342. The pathogenic effects of all three revertants were also determined on 4-week-old BALB/c mice. After intracerebral infection with 100 PFU of the revertants or wild-type virus, mice died within 6 days, whereas groups of four mice inoculated with PBS or 100,000 PFU of *ts*342 survived.

DISCUSSION

Our results show that the reduced pathogenicity of *ts*342 correlates well with its restricted replication in astrocytes. It is remarkable that the *ts* lesion in the viral genome leads to a restricted MHV infection only in concordance with host-cell factors contributed by the astrocyte. More experiments are now needed to determine at the molecular level how exactly the *ts* lesion of mutant *ts*342 causes reduced pathogenicity and restricted replication in astrocytes. The results of our electron microscopic and biochemical studies indicate that there is a maturation defect, probably caused by a lack of viral glycoproteins. MHV-A59 acquires its envelope by budding at membranes inside the cell, specifically the endoplasmic reticulum, rather than at the plasma membrane (5, 33). This site of budding is determined by the envelope glycoprotein E1, which accumulates in internal membranes after its synthesis and is only transported out of the cell as part of virus. The other viral glycoprotein, E2, is, although essential for infectivity, not needed for virus maturation (12, 24). Since mRNAs 3 and 6 coding for E2 and E1, respectively, were present normally in *ts*342-infected astrocytes, either one or both mRNAs are not functional or the glycoproteins are rapidly degraded. At this moment it is unclear how a mutation causing a defect in RNA synthesis at 40°C would lead to either of these possibilities.

We compared our data with those of others who have studied the replication of viruses in cells of the central nervous system to see whether we could detect a general

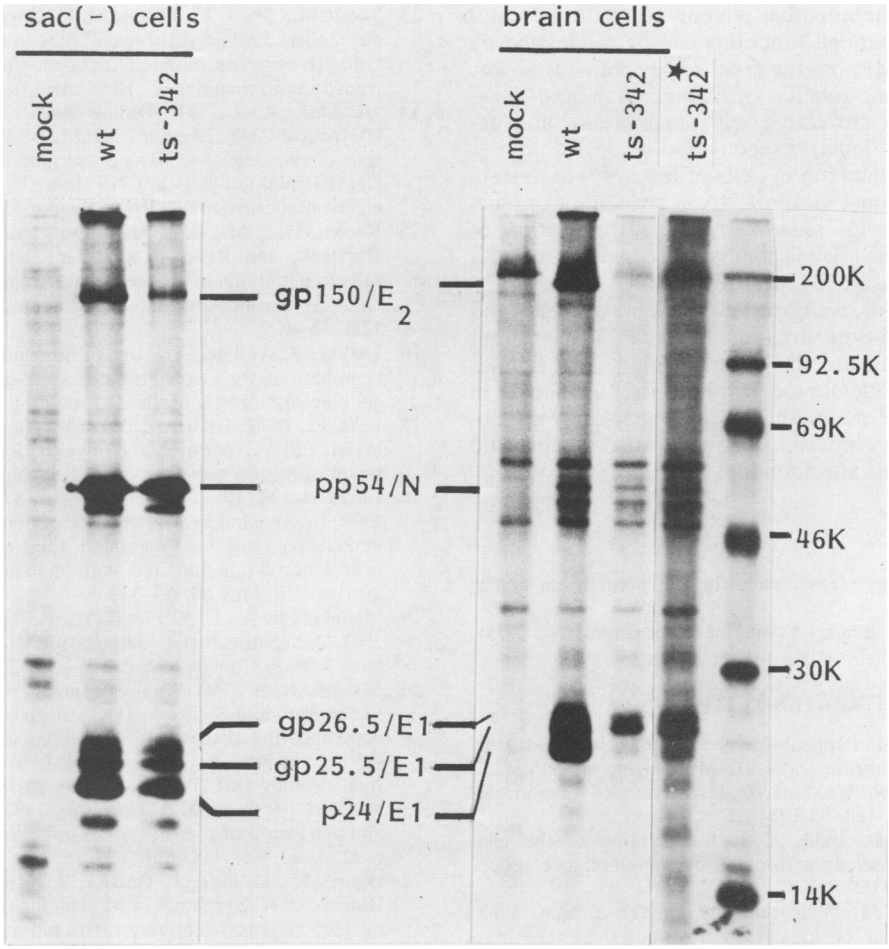

FIG. 5. Virus-specific proteins present in Sac(−) cells and mouse brain astrocytes infected with wild-type (wt) MHV-A59 or its mutant *ts*342. Cells were labeled with [^{35}S]methionine. Virus-specific proteins immunoprecipitated from the cell lysates with mouse anti-MHV serum were analyzed by polyacrylamide gel electrophoresis. The intracellular virus-specific proteins and molecular weight markers are indicated. The number of counts in the sample from wild type-infected brain cells was 57,500 compared with 19,000 for *ts*342-infected astrocytes. To compare the same number of counts of both virus strains, a threefold-longer exposure (6 days) of the *ts*342 sample is also included (ts-342*). K, 10^3.

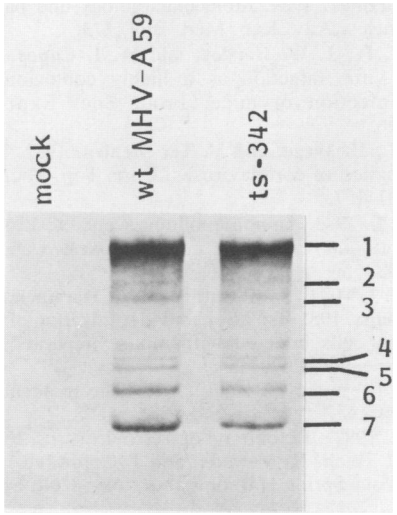

pattern in the interaction between these cells and viruses. This seems indeed to be the case. A selective lack of synthesis of the M (matrix) protein causes restricted replication of measles and Sendai viruses (3, 8, 22). Also, the replication of Sendai virus in rat glial cells is only restricted at high temperature (22). In a nonproductive infection of rubella virus in rat glial cells, two viral proteins are lacking (23).

Regarding the *ts* mutation in the viral genome and host-cell factors acting in concert, the results of Lucas et al. (18) are relevant. They described continuous cell lines of neural origin persistently infected with strains of MHV or measles virus. Virus replication in these cultures was thermosensitive. Progeny virus, however, was thermostable when tested in indicator cell lines. This means that a host-cell mecha-

FIG. 6. Analysis of virus-specific RNAs present in mouse brain astrocytes infected with wild-type (wt) MHV-A59 or *ts*342. Lysates of actinomycin D-treated, [^{3}H]uridine-labeled cells were phenol extracted; the RNAs were ethanol precipitated and analyzed by agarose gel electrophoresis. The virus-specific RNAs 1 to 7 are indicated.

nism(s) determines the eventual phenotype of the *ts* mutation. The relevant host-cell functions can be modulated by the level of cyclic AMP, but the results are confusing so far. In measles virus- and rubella virus-infected neural cells, restricted replication correlated with an increase and decrease in cyclic AMP level, respectively (21, 35).

Defective virus replication in cells of the nervous system owing to a nonfunctional viral mRNA is not without precedence. Carter et al. (3) have shown that replication of measles virus in an SSPE cell line is the consequence of a nonfunctional mRNA for the viral M protein.

Like others (5, 6, 34), we observed tubular structures and tubular bodies in wild-type virus-infected cells. It seems that MHV is able to stimulate the differentiation of a cellular system resulting in membrane proliferation. Although in mutant-infected cells no mature virus particles were observed, membrane proliferation in the form of sheets and spherical particles was still found.

ACKNOWLEDGMENTS

We thank Maud Maas Geesteranus for the preparation of the manuscript.

We thank the Prinses Beatrix Fonds for support (grant 82-2035).

LITERATURE CITED

1. **Bailey, O. T., A. M. Pappenheimer, F. S. Cheever, and J. B. Daniels.** 1949. A murine virus (JHM) causing disseminated encephalomyelitis with extensive destruction of myelin. II. Pathology. J. Exp. Med. **90**:195–212.
2. **Bignami, A., and D. Dahl.** 1972. Localization of the glial fibrillary acidic protein in astrocytes by immunofluorescence. Brain Res. **43**:429–435.
3. **Carter, M. J., M. M. Willcocks, and V. Ter Meulen.** 1983. Defective translation of measles virus matrix protein in a subacute sclerosing panencephalitis cell line. Nature (London) **305**:153–155.
4. **Cheever, F. S., J. B. Daniels, A. M. Pappenheimer, and O. T. Bailey.** 1949. A murine virus (JHM) causing disseminated encephalomyelitis with extensive destruction of myelin. I. Isolation and biological properties of the virus. J. Exp. Med. **90**:181–194.
5. **David-Ferreira, J. F., and R. A. Manaker.** 1965. An electron microscope study of the development of a mouse hepatitis virus in tissue culture cells. J. Cell Biol. **24**:57–78.
6. **Dubois-Dalcq, M. E., E. W. Doller, M. V. Haspel, and K. V. Holmes.** 1982. Cell tropism and expression of mouse hepatitis viruses (MHV) in mouse spinal cord cultures. Virology **119**:317–331.
7. **Fujiwara, K., S. Takenaka, and S. Shumiya.** 1976. Carrier state of antibody and viruses in a mouse breeding colony persistently infected with Sendai and mouse hepatitis viruses. Lab. Anim. Sci. **26**:153–159.
8. **Hall, W. W., and P. W. Choppin.** 1979. Evidence for lack of synthesis of the M-polypeptide of measles virus in brain cells in subacute sclerosing panencephalitis. Virology **99**:443–447.
9. **Hansson, E.** 1984. Cellular composition of a cerebral hemisphere primary culture. Neurochem. Res. **9**:153–172.
10. **Haspel, M. V., P. W. Lampert, and M. B. Oldstone.** 1978. Temperature-sensitive mutants of mouse hepatitis virus produce a high incidence of demyelination. Proc. Natl. Acad. Sci. USA **75**:4033–4036.
11. **Holland, J., K. Spindler, F. Horodyski, E. Grabau, S. Nichol, and S. Vandepol.** 1982. Rapid evolution of RNA genomes. Science **215**:1577–1585.
12. **Holmes, K., E. W. Doller, and L. S. Sturman.** 1981. Tunicamycin resistant glycosylation of a coronavirus glycoprotein: demonstration of a novel type of viral glycoprotein. Virology **115**:334–344.
13. **Jacobs, L., W. J. M. Spaan, M. C. Horzinek, and B. A. M. van der Zeijst.** 1981. Synthesis of subgenomic mRNAs of mouse hepatitis virus is initiated independently: evidence from UV transcription mapping. J. Virol. **39**:401–406.
14. **Knobler, R. L., M. Dubois-Dalcq, M. V. Haspel, A. P. Claysmith, P. W. Lampert, and M. B. A. Oldstone.** 1981. Selective localization of wild type and mutant mouse hepatitis virus (JHM strain) antigens in CNS tissue by fluorescence, light and electron microscopy. J. Neuroimmunol. **1**:81–92.
15. **Koolen, M. J. M., A. D. M. E. Osterhaus, G. van Steenis, M. C. Horzinek, and B. A. M. van der Zeijst.** 1983. Temperature-sensitive mutants of mouse hepatitis virus strain A59: isolation, characterization and neuropathogenic properties. Virology **125**:393–402.
16. **Laskey, R. A.** 1980. The use of intensifying screens or organic scintillations for visualizing radioactive molecules resolved by gel electrophoresis. Methods Enzymol. **65**:363–371.
17. **Lavi, E., D. H. Gilden, Z. Wroblewska, L. B. Rorke, and S. R. Weiss.** 1984. Experimental demyelination produced by the A59-strain of mouse hepatitis virus. Neurology **34**:597–603.
18. **Lucas, A., M. Coulter, R. Anderson, S. Dales, and W. Flintoff.** 1978. In vivo and in vitro models of demyelinating diseases. II. Persistence and host-regulated thermosensitivity in cells of neural derivation infected with mouse hepatitis and measles viruses. Virology **88**:325–337.
19. **Manaker, R. A., C. V. Piczak, A. A. Miller, and M. F. Stanton.** 1961. A hepatitis virus complicating studies with mouse leukemia. J. Natl. Cancer Inst. **27**:29–45.
20. **Massalski, A., M. Coulter-Mackie, R. L. Knobler, M. J. Buchmeier, and S. Dales.** 1982. In vivo and in vitro models of demyelinating diseases. V. Comparison of the assembly of mouse hepatitis virus, strain JHM, in two murine cell lines. Intervirology **18**:135–146.
21. **Miller, C. A., and D. R. Carrigan.** 1982. Reversible repression and activation of measles virus infection in neural cells. Proc. Natl. Acad. Sci. USA **79**:1629–1633.
22. **Ogura, H., H. Sato, J. Tanaka, S. Kamija, T. Yoshie, and M. Hatano.** 1984. Synthesis of M proteins of HVJ (Sendai virus) in rat glial cells is selectively restricted at a non-permissive temperature. J. Gen. Virol. **65**:639–643.
23. **Pope, D. D., and D. van Alstyne.** 1981. Evidence for restricted replication of rubella virus in rat glial cells in culture. Virology **113**:776–780.
24. **Rottier, P. J. M., M. C. Horzinek, and B. A. M. van der Zeijst.** 1981. Viral protein synthesis in mouse hepatitis virus strain A59-infected cells: effects of tunicamycin. J. Virol. **40**:350–357.
25. **Rottier, P. J. M., W. J. M. Spaan, M. C. Horzinek, and B. A. M. van der Zeijst.** 1981. Translation of three mouse hepatitis virus strain A59 subgenomic RNAs in *Xenopus laevis* oocytes. J. Virol. **38**:20–26.
26. **Rottier, P. J. M., B. A. M. van der Zeijst, W. J. M. Spaan, and M. C. Horzinek.** 1984. Molecular biology and pathogenesis of coronaviruses. Adv. Exp. Med. Biol. **173**.
27. **Rowe, W. P., J. W. Hartley, and W. I. Capps.** 1963. Mouse hepatitis virus infection as a highly contagious, prevalent, enteric infection of mice. Proc. Soc. Exp. Biol. Med. **112**:161–165.
28. **Siddell, S., H. Wege, and V. Ter Meulen.** 1982. The structure and replication of coronaviruses. Curr. Top. Microbiol. Immunol. **99**:131–157.
29. **Smith, A. L.** 1983. An immunofluorescence test for detection of serum antibody to rodent coronaviruses. Lab. Anim. Sci. **33**:157–160.
30. **Spaan, W. J. M., P. J. M. Rottier, M. C. Horzinek, and B. A. M. van der Zeijst.** 1981. Isolation and identification of virus-specific mRNAs in cells infected with mouse hepatitis virus (MHV-A59). Virology **108**:424–434.
31. **Sturman, L., and K. Holmes.** 1983. The molecular biology of coronaviruses. Adv. Virus Res. **28**:35–111.
32. **Teich, N.** 1982. Taxonomy of retrovirus, p. 205–208. *In* R. Weiss, N. Teich, H. Varmus, and J. Coffin (ed.), RNA tumor viruses. Cold Spring Harbor Laboratory, Cold Spring Harbor, N.Y.

33. **Ter Meulen, V., S. Siddell, and H. Wege.** 1981. Biochemistry and biology of coronaviruses. Adv. Exp. Med. Biol. **142**.
34. **Tooze, J., S. Tooze, and G. Warren.** 1984. Replication of coronavirus MHV-A59 in Sac− cells: determination of the first site of budding of progeny virions. Eur. J. Cell Biol. **33**:281–293.
35. **van Alstyne, D., and D. N. Paty.** 1983. The effect of dibutyryl cyclic AMP on restricted replication of rubella virus in rat glial cells in culture. Virology **124**:173–180.
36. **Wege, H., S. Siddell, and V. Ter Meulen.** 1982. The biology and pathogenesis of coronaviruses. Curr. Top. Microbiol. Immunol. **99**:165–200.
37. **Weiland, E., M. Mussgay, and F. Weiland.** 1978. Non-producer malignant tumor cells with rescuable sarcoma virus genome isolated from a recurrent Moloney sarcoma. J. Exp. Med. **148**:408–423.